

Table I. Kinetic Data for Substitution of L at $\text{Ru}(\text{NH}_3)_5(\text{H}_2\text{O})^{2+}$ in Nafion at 25 °C

	k_{activity}^a , $\text{M}^{-1} \text{s}^{-1}$	partition coefficient [L] _{solution} = 0.1 M	$k_{\text{intrinsic}}^b$, $\text{M}^{-1} \text{s}^{-1}$	$k_{\text{H}_2\text{O}}$, $\text{M}^{-1} \text{s}^{-1}$	ΔH^\ddagger , ^d kcal/mol	$\Delta H^\ddagger_{(\text{H}_2\text{O})}$, kcal/mol	ΔS^\ddagger , eu ^d	$\Delta S^\ddagger_{(\text{H}_2\text{O})}$, eu
isonicotinamide	0.20	5.0	0.041	0.105 ^c	14.8		-15.2	
pyridine	0.77	7.0	0.11	0.093 ^c	15.1	16.9 ^c	-12.0	-6.6 ^c
4-pyridylcarbinol	0.48	6.9	0.070	0.082 ^e	14.2	17.3 ^e	-16.4	-5.6 ^e

^a Bimolecular rate constant calculated at 0.10 M solution concentration of L. ^b Partition corrected rate constant. ^c Values are from ref 5a. ^d Measured over 5–45 °C; eu = cal mol⁻¹ deg⁻¹. ^e This work.

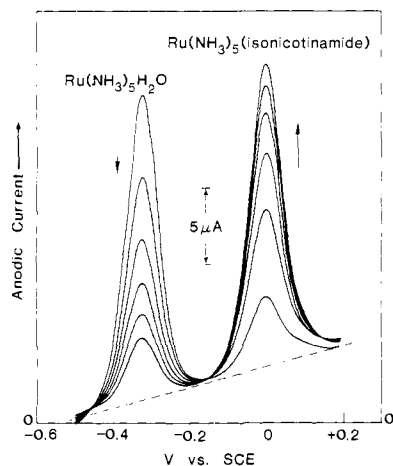


Figure 1. Substitution reaction of isonicotinamide with Nafion-bound $\text{Ru}(\text{NH}_3)_5(\text{H}_2\text{O})^{2+}$, as monitored with linear-sweep voltammetry. The scans (200 mV/s sweep rate) were made at 20-s intervals; the potential between scans was maintained at -0.6 V vs. SCE. The dashed line represents background current at the Nafion-coated pyrolytic graphite surface in aqueous solution.

our system is very low, and an upper limit on the activity is estimated as $0.029 \text{ M}^{-1} \text{ s}^{-1}$. This indicates a change of greater than 10^2 in the selectivity of Ru(II) for pyridine vs. $\text{NC}_5\text{H}_4\text{COO}^-$ from aqueous media to the Nafion phase.

The full width at half-maximum of the voltammetric waves (approximately 120 mV) for both the reactant and product does not vary with the extent of reaction, implying that the electrochemically detectable Ru(II) sites react with comparable rates on our reaction time scale. Additionally, the rates are independent of polymer thickness (0.2–0.8 μm ; constant $\text{Ru}(\text{NH}_3)_5(\text{H}_2\text{O})^{2+}$ film concentration), indicating that the substitution rates are not limited by substrate diffusion into the polymer phase. Substantial contribution from the poorly ligating, protonated pyridinium ions^{5a} is excluded because the partition coefficients and substitution activities were determined to be independent of pH in our measurement range (typically $\text{pH} > \text{p}K_{\text{ligand}} + 2$).

A direct comparison of intrinsic rates requires measurement of the actual concentration of ligand within the polymer film. Partition coefficients for L are found to vary with ligand polarity, and for a given L they are also dependent on its solution concentration. Utilizing the partition coefficient data, we find a first-order dependence of the substitution rate on the concentration of ligand inside the Nafion film. A summary of our kinetic data for the substitution of three pyridine ligands is given in Table I. A striking feature of these results is the contrast between the essentially constant reaction rate for substitution of the $\text{Ru}(\text{NH}_3)_5(\text{H}_2\text{O})^{2+}$ ion with functionalized pyridine ligands in aqueous solution^{5,10} and the variation of reaction rate constants when the Ru(II) ion is immobilized in Nafion films.

Examination of ΔH^\ddagger and ΔS^\ddagger (Table I) for the substitution reactions of the three ligands indicates that the differences in intrinsic reactivity from the polymer and solution data are primarily due to an entropic effect. It is likely that the significant difference between the two dipolar pyridines and pyridine itself results from the greater interactions (hydrogen bonding, elec-

trostatic) possible between these two functionalized ligands and the Nafion environment. Exploitation of these interactions may thus lead to reactivity of polymer-bound reagents which is different than observed in aqueous solutions.

Acknowledgment. We acknowledge helpful discussions with Dr. W. Tumas and Profs. J. I. Brauman and H. Taube of Stanford University. Support for this work was provided by the Gas Research Institute. N.S.L. also received support from an IBM Young Faculty Development Award and from the Exxon Educational Foundation, Mobil Co., and Monsanto Co. under the Presidential Young Investigator Program.

Tetraaryldiphosphine Cation Radicals. Electrochemical Generation and ESR Study

Marcel Culcasi, Gérard Gronchi, and Paul Tordo*

*Laboratoire de Structure et Réactivité des
Espèces Paramagnétiques, CNRS UA 126
Université de Provence
and the Laboratoire de
l'Ecole Supérieure de Chimie de Marseille
13397 Marseille Cedex 13, France*

Received July 17, 1985

Tetraaryl-¹ and tetraalkylhydrazine² cation radicals have been extensively studied. These cation radicals prefer planar, olefin-like geometries, with coplanar p-rich lone pair orbitals forming a delocalized or a localized three-electron bond. In the case of tetraalkylhydrazine cation radicals, pyramidalization at nitrogen is relatively facile, and sterically constrained examples of these radicals can exist either in an "anti-bent" or a "syn-bent" configuration, the former being slightly more stable due to a more favorable σ, π orbital mixing.³

In agreement with the experimental results, theoretical calculations² predict the hydrazine cation radical to be planar or very nearly so, depending on the theoretical level used, with a rotation barrier of 31 kcal/mol. The N–N bond in the cation radical (1.292 Å) is calculated to be significantly shorter than that in hydrazine itself (1.413 Å). Therefore, H_2NNH_2^+ behaves as a typical two-center π bond with about half the π bond energy of ethylene. Since the nitrogen atoms are pyramidal in the preferred conformer of tetraalkylhydrazines, it is clear that in the corresponding cation radicals the energy required to make the nitrogen centers planar is largely compensated for by three-electron π stabilization.

Tricoordinate atoms in the second row of the periodic table are more highly pyramidalized than their first-row counterparts.⁴ On the other hand, the bond energy of a typical two-center P–P π bond is small, and diphosphenes can be isolated only if they are kinetically stabilized by large steric crowding.⁵

(1) Cauquis, G.; Delhomme, H.; Serve, D. *Electrochim. Acta* **1975**, *12*, 1019. Fomin, G. V.; Ivanov, Yu. A.; Shaprov, A. B.; Solotov, A. N.; Pirozhkov, S. D.; Rozantsev, E. G. *Izv. Akad. Nauk. SSSR Ser. Khim.* **1978**, *7*, 1626.

(2) Nelsen, S. F. *Acc. Chem. Res.* **1981**, *14*, 131. Nelsen, S. F.; Cunkle, G. T.; Evans, D. H.; Clark, T. *J. Am. Chem. Soc.* **1983**, *105*, 5928.

(3) Nelsen, S. F.; Blackstock, S. C.; Yumibe, N. P.; Frigo, T. B.; Carpenter, J. E.; Weinhold, F. *J. Am. Chem. Soc.* **1985**, *107*, 143.

(4) Cherry, W.; Epiotis, N.; Borden, W. T. *Acc. Chem. Res.* **1977**, *10*, 167.

(10) Shepherd, R. E. Ph.D. Thesis, Stanford University, Stanford, CA, 1971.

Table I. Electrochemical^a Oxidation of Tetraaryldiphosphines

compd	$E_p(a)$, V ^b	$E_p(c)$, V ^c	$I_p(c)/I_p(a)$ ^d
1	0.795	0.715	0.92
2	0.718	0.599	0.95
3	0.592	0.477	1.00
(Mes) ₃ P ^e	0.784	0.680	0.87
(Xy) ₃ P ^e	0.885	0.792	1.00

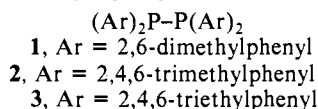
^aCyclic voltammetry ($v = 100$ mV/s) at a stationary platinum electrode in butyronitrile containing 0.1 M tetra-*n*-butylammonium hexafluorophosphate. ^bAnodic peak potential vs. SCE. ^cCathodic peak potential vs. SCE. ^dRatio of peak currents. ^eMes = 2,4,6-trimethylphenyl and Xy = 2,6-dimethylphenyl; see ref 12.

Table II. ESR Features^a of Cation Radicals of Tetraaryldiphosphines

radical	a_p , G ^b	g	T , K
1⁺	171	2.0060	291
2⁺	170	2.0063	290
3⁺	175	2.0061	293
(Mes) ₃ P ^{+,c}	240	2.0052	293
(Xy) ₃ P ^{+,c}	244	2.0052	288

^aIn butyronitrile containing 0.1 M tetra-*n*-butylammonium hexafluorophosphate. ^bObtained by using the Breit Rabi equation. ^cMes = 2,4,6-trimethylphenyl and Xy = 2,6-dimethylphenyl.

Considering these fundamental differences between nitrogen and phosphorus compounds, it is very interesting to investigate the electronic structure of the phosphorus analogues of hydrazine cation radical. The recent publication⁶ of ab initio calculations on the diphosphine cation radical (P₂H₄⁺) prompts us to report our preliminary results on the electrochemical oxidation of sterically crowded tetraaryldiphosphines **1**, **2**, and **3** and the liquid



solution ESR study of the ensuing cation radicals **1⁺**, **2⁺**, and **3⁺**.

The cyclic voltammetry study of diphosphines **1–3** showed a single-electron reversible (or nearly reversible) oxidation at room temperature; the anodic and cathodic peak potential values are listed in Table I. The ensuing cationic species are relatively persistent, as shown by the close values of the anodic and cathodic peak currents. However, the half-lives of these cationic species depend directly upon the bulk of the phosphorous ligands, and under the same conditions, tetraphenyldiphosphine showed a completely irreversible oxidation process.

When the oxidation of **1**, **2**, or **3** was performed in the cavity of an ESR spectrometer, in each case a four-line spectrum assigned to **1⁺**, **2⁺**, or **3⁺** was observed in the temperature range -40 to $+50$ °C (Figure 1). The ESR features of cation radicals **1⁺**, **2⁺**, and **3⁺** are listed in Table II.

In a first-order approximation, coupling to two equivalent phosphorus nuclei yields a three-line (1:2:1) ESR spectrum. In the case of **1⁺**, **2⁺**, or **3⁺**, because of the large magnitude of the phosphorus hyperfine splitting, the $M_I = 0$ transition appeared as a doublet corresponding to $I = 0$ or 1, that is, to the singlet or the triplet state, respectively, of the two coupled phosphorus nuclei. The separation between the (0,0) transition and the (1,0) transition which appears at lower magnetic field is given by $(a_p)^2/H$, where H is the magnetic field corresponding to the position of the (1,0) transition.⁷ For radicals **1⁺**, **2⁺**, and **3⁺**, the second-order splitting was resolved and the calculated values

**Figure 1.** ESR spectrum of tetrakis(2,4,6-triethylphenyl)diphosphine cation radical (**3⁺**) electrogenerated in butyronitrile 0.1 M in tetra-*n*-butylammonium hexafluorophosphate at 296 K.

were very close to the experimental values (for **1⁺**, $a_p^2/H_{(\text{calcd})} = 9.06$ G and $a_p^2/H_{(\text{exptd})} = 10.0$ G).

Very similar ESR spectra were observed for a series of phosphine dimer cation radicals (X₃PPX₃)⁺ produced during the electrochemical oxidation of different trivalent phosphorus compounds.⁸

For the three cation radicals investigated, the four lines of their ESR spectra were of unequal width (Figure 1), but no significant temperature-dependent line-width effect was observed in the range -40 to $+50$ °C. The line-width effect was interpreted in terms of the nuclear spin relaxation induced by the time-dependent anisotropic dipolar phosphorus interaction. The semiclassical density matrix theory, as discussed for ESR by Freed and Fraenkel,⁹ was successfully applied to calculate the intensity ratio of the different lines.¹⁰

The large phosphorus splitting observed for radicals **1⁺**, **2⁺**, or **3⁺** clearly indicates that the phosphorus centers are highly pyramidal. The P_{3s} orbital population derived from the a_p values is close to 9%. This mean value is significantly higher than that of close to 6.5% observed for the corresponding triaryldiphosphine cation radicals (Table II) which are thus expected to be less bent at phosphorus.

Owing to the large value of the PP bond distance (2.1–2.2 Å),¹¹ a symmetric tetraaryldiphosphine bearing bulky aryl substituents is expected to be sterically less constrained and thus more bent at the phosphorus center than the corresponding triaryldiphosphine, and this difference is retained in the corresponding cation radicals.

Our experimental results are in agreement with the theoretical calculations⁶ on P₂H₄⁺, which predicted that the energy required to make the two phosphorus centers planar is too large to be compensated by any three-electron stabilization. As pointed out by Clark,⁶ P₂H₄⁺ is nevertheless strongly stabilized relative to PH₃⁺. The adiabatic ionization potential of diphosphine is calculated to be 0.92 eV lower than that of PH₃. On the other hand, coulometric and ESR experiments¹² clearly indicate that the diphosphine cation radicals have longer half-lives than the corresponding phosphine cation radicals.

Finally, it is worth noting that the absence of a significant temperature-dependent line-width effect for **1⁺**, **2⁺**, and **3⁺** suggests that these radicals have electronically delocalized

(5) Yoshifuji, M.; Shima, I.; Inamoto, N. *J. Am. Chem. Soc.* **1981**, *103*, 4587. Bertrand, G.; Couret, C.; Escudie, J.; Majid, S.; Majoral, J. P. *Tetrahedron Lett.* **1982**, *23*, 3567. Couret, C.; Escudie, J.; Satge, J. *Tetrahedron Lett.* **1982**, *23*, 4941. Cowley, A. H.; Kilduff, J. E.; Newman, T. H.; Pakulski, M. *J. Am. Chem. Soc.* **1982**, *104*, 5820. Review: Cowley, A. H. *Polyhedron* **1984**, *3*, 389.

(6) Feller, D.; Davidson, E. R.; Borden, W. T. *J. Am. Chem. Soc.* **1985**, *107*, 2596. Clark, T. *J. Am. Chem. Soc.* **1985**, *107*, 2597.

(7) Fessenden, R. W. *J. Chem. Phys.* **1962**, *37*, 747.

(8) Gara, W. B.; Roberts, B. P. *J. Chem. Soc., Perkin Trans. 2* **1978**, 150.

(9) Freed, J. H.; Fraenkel, G. *J. Chem. Phys.* **1963**, *39*, 326.

(10) The hyperfine tensors were assumed to be of cylindrical symmetry around the directions of the phosphorus lone pairs. The adiabatic contribution to the line width was then considered to be predominant and was calculated as a function of α , the angle between the directions of the lone pairs. A good fit between the calculated and the experimental line widths was obtained for a value of α close to 36°. Ayant, Y.; Tordo, P., unpublished results.

(11) McAdam, A.; Beagley, B.; Hewitt, T. G. *Trans. Faraday Soc.* **1970**, *66*, 2732. Richter, R.; Kaiser, J.; Sieler, J.; Hartung, H.; Peter, C. *Acta Crystallogr., Sect. B* **1977**, *B33*, 1887.

(12) Culcasi, M.; Gronchi, G.; Tordo, P., unpublished results.

structures with a C_{2h} symmetry rather than localized electronic structures with different bending at phosphorus.

The electrochemical oxidation of different diphosphines is under investigation in order to get more information concerning the mechanism of stabilization of the corresponding cation radicals and their reactivity.

Acknowledgment. We thank the Centre National de la Recherche Scientifique (UA 126) and the LETI (CEA, Grenoble) for financial support and Pr. Y. Ayant for helpful discussion.

High-Resolution NMR with a Surface Coil

M. Gochin* and A. Pines*

Department of Chemistry, University of California
Berkeley, and Materials and Molecular
Research Division, Lawrence Berkeley Laboratory
Berkeley, California 94720

Received May 29, 1985

Topical nuclear magnetic resonance is a method by which chemical shift spectra are obtained from a spatially selected region inside an intact system. Surface coils have been widely used for attaining spatial selectivity, by taking advantage of the strongly varying rf intensity at different distances from the coil.¹⁻⁹ Frequency resolution in this type of spectroscopy and related volume-selective approaches^{10,11} remains a serious problem, which is typically overcome by shimming the magnet for each NMR region being observed or moving the sample so that the observed region lies in a preset homogeneous spot of the magnet.¹⁰

In this paper we demonstrate the first application of SHARP NMR spectroscopy¹² to obtain high-resolution heteronuclear NMR spectra in an inhomogeneous field with a surface coil. This method employs the detection of single-quantum echoes with coherence transfer methods¹³⁻¹⁶ or heteronuclear echoes¹² in double-quantum^{16,17} evolution. It eliminates the need for shimming altogether, yielding very sharp lines close to the frequency of the heteronuclear spins. Figure 1 shows an illustrative SHARP spectrum of ethanol in an inhomogeneous field and compares it to the normal ^{13}C and ^1H spectra. The narrow lines and high sensitivity of SHARP greatly enhance the applicability of surface coil and volume selective NMR to nonhomogeneous samples.

The pulse sequence used here for the case of ^{13}C (S) and ^1H (I) is illustrated in Figure 2. The concept is the generation of signal as a function of an evolution time, t_1 , which contains chemical shift information but has field inhomogeneity effects

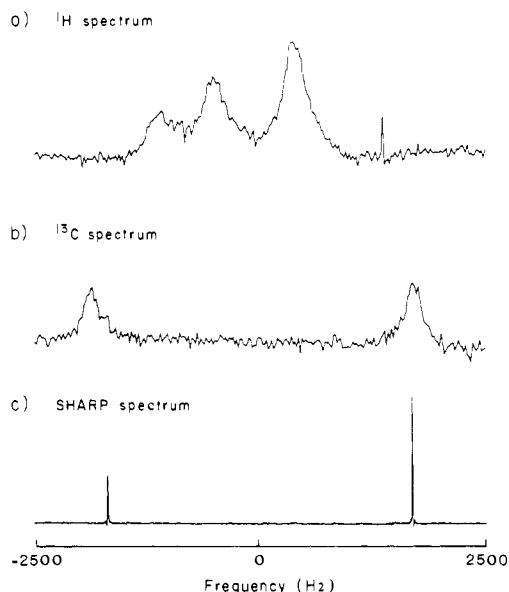


Figure 1. Surface coil spectra of a 2-mm bulb sample of ethanol, enriched to 25% in ^{13}C at each position, one ^{13}C per molecule. (a) ^1H spectrum (1 min); (b) ^{13}C spectrum with 10-ms proton presaturation and proton decoupling (2 h); (c) SHARP spectrum obtained by the method of Figure 2 and with the spectrometer phase inverted, to give $\delta = (\delta_C - \delta_H)/4$ (1 h). Spectra were taken on a 360-MHz spectrometer.

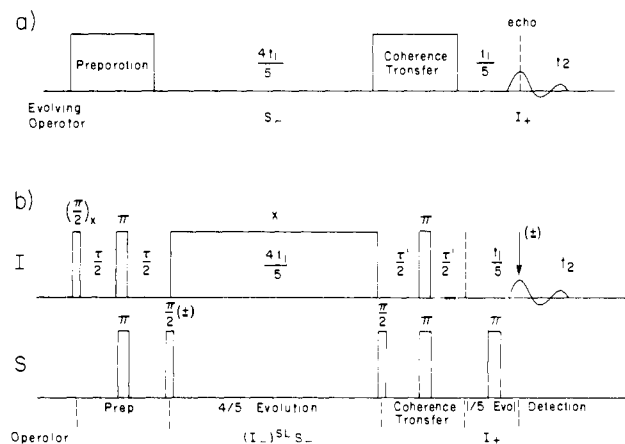


Figure 2. Pulse sequence used for SHARP spectra. (a) Schematic sequence showing a period of proton-decoupled S-spin evolution, followed by a proton evolution period $1/4$ as long. (b) Details of the coherence transfer steps between protons and S spins. Preparation times τ , τ' were chosen to be equal to $1/2J_{IS}$. A constant purging pulse of 8 ms was used before the evolution period to dephase unwanted nonsatellite magnetization. The symbols $\pi/2$ (\pm) and \downarrow (\pm) indicate that two experiments differing in phase by 180° are subtracted on alternate shots to further suppress nonsatellite signal.

completely removed. This can be achieved by noting that $\gamma_H/\gamma_C = 3.997 \approx 4$, so that proton nuclei will dephase (or rephase) about 4 times as rapidly as carbon nuclei in a given magnetic field. Thus, by allowing ^{13}C to dephase for $4t_1/5$ and ^1H to rephase for $t_1/5$, an echo is produced at the end of t_1 . The sequence in Figure 2 has precisely this effect, with the added feature that magnetization is both initiated and detected in the proton spin system, hence maximizing sensitivity. Thus, there are two coherence transfer steps, one to prepare, from I_x , heteronuclear double-quantum coherence, $I_x S_x$, and the second to transfer coherence back to I_x for eventual detection. The data are collected point-by-point and Fourier transformed with respect to $4t_1/5$. The chemical shifts are given by

$$\delta = -\delta_C + \delta_H/4$$

Heteronuclear coupling is completely removed, while homonuclear coupling is scaled by $1/4$ and is not resolved in Figure 1. Thus,

(1) Gadian, D. G. "Nuclear Magnetic Resonance and Its Applications to Living Systems"; Oxford University Press: Oxford, 1982.

(2) Ackerman, J. J. H.; Grove, T. H.; Wong, G. G.; Gadian, D. G.; Radda, G. K. *Nature (London)* **1980**, *283*, 167.

(3) Bendall, M. R.; Gordon, R. E. *J. Magn. Reson.* **1983**, *53*, 365.

(4) Bendall, M. R. *Chem. Phys. Lett.* **1983**, *99*, 310.

(5) Haase, A.; Malloy, C.; Radda, G. K. *J. Magn. Reson.* **1983**, *55*, 164.

(6) Bendall, M. R.; Pegg, D. T. *J. Magn. Reson.* **1984**, *57*, 337.

(7) Bottomley, P. A.; Foster, T. B.; Darrow, R. D. *J. Magn. Reson.* **1984**, *59*, 338.

(8) Shaka, A. J.; Freeman, R. *J. Magn. Reson.* **1984**, *59*, 169.

(9) Baum, J.; Tycko, R.; Pines, A. *J. Am. Chem. Soc.*, in press.

(10) Aue, W. P.; Muller, S.; Cross, T. A.; Seelig, J. *J. Magn. Reson.* **1984**, *56*, 350.

(11) Aue, W. P.; Muller, S.; Seelig, J. *J. Magn. Reson.* **1985**, *61*, 392.

(12) Gochin, M.; Weitekamp, D. P.; Pines, A. *J. Magn. Reson.* **1985**, *63*, 431.

(13) Maudsley, A. A.; Wokaun, A.; Ernst, R. R. *Chem. Phys. Lett.* **1978**, *55*, 9.

(14) Maudsley, A. A.; Ernst, R. R. *Chem. Phys. Lett.* **1977**, *50*, 368.

(15) Weitekamp, D. P.; Garbow, J. R.; Murdoch, J. B.; Pines, A. *J. Am. Chem. Soc.* **1981**, *103*, 3578. Garbow, J. R.; Weitekamp, D. P.; Pines, A. *J. Chem. Phys.* **1983**, *79*, 5301.

(16) Muller, L. *J. Am. Chem. Soc.* **1979**, *101*, 4481.

(17) Bax, A.; Griffey, R. H.; Hawkins, B. L. *J. Magn. Reson.* **1983**, *55*, 301.